This is the Pre-Published Version.

Z. Liang, S. Lin, X. Huang (2022) *Smoldering Ignition and Emission Dynamics of Wood under Low Irradiation,* **Fire and Materials**. https://doi.org/10.1002/fam.3107

Smoldering Ignition and Emission Dynamics of Wood under Low Irradiation

Zhirong Liang [1,#], Shaorun Lin[1,2,#], Xinyan Huang[1,*]

[1]*Research Centre for Fire Safety Engineering, Department of Building Environment and Energy Engineering, The Hong Kong Polytechnic University, Kowloon, Hong Kong*

[2]*The Hong Kong Polytechnic University Shenzhen Research Institute, Shenzhen, China*

[#]Joint first author, these authors contributed equally to this study.

*Corresponding to xy.huang@polyu.edu.hk (X. Huang)

Abstract: Wood is one of the longest-standing and sustainable construction and building materials, and has gained a new renaissance for high-rise buildings to achieve global carbon neutrality. However, wood can sustain both flaming and smoldering fires, and numerous timber structure fires have raised fire safety to be a public concern. This work investigates the smoldering ignition of wood blocks under long-lasting low-intensity irradiation and the robustness of smoldering fire after the removal of irradiation. We found a smoldering ignition map including three regimes, (I) no ignition, (II) unsustained smoldering, and (III) self-sustained smoldering. The minimum irradiation for smoldering ignition of wood is about 5.5 kW/m^2 after heating for hours. Without sufficient and in-depth preheating, smoldering ignition cannot self-sustain without irradiation. The criteria for self-sustained smoldering on thick wood include the minimum surface temperature of 350±20 ºC, the minimum smoldering front thickness of 30 ± 5 mm, and the minimum mass flux of 3.8 ± 0.4 g/m^2-s before the irradiation is terminated. The CO/CO_2 ratio of the smoldering wood under low irradiation varies between 0.1 and 0.2. This work helps evaluate the fire risk of wood materials and understand their burning behaviors under real fire scenarios.

Keywords*: Smouldering combustion; Ignition map; Smoldering limit; External radiation; Timber fire*

1. Introduction

Wood has been used as one of the longest-standing construction and building materials (timber) for over 10,000 years[1,2], and has contributed significantly to the history of human civilization. For example, the Neolithic Long House (Fig. 1a), was a long and narrow timber dwelling in Europe beginning at least as early as the period 5000 to 6000 BC[3]. In the 21st century, wood has gained a new renaissance as a sustainable construction material for high-rise buildings to achieve carbon neutrality globally, and the mechanical performance of wood or wooden material has been well improved by the development of mass timber elements such as cross-laminated timber (CLT) panels for use in advanced engineering structures and applications[4–6]. For example, the Brock Commons Tallwood House (Fig. 1b), an 18-

storey student residence at the University of British Columbia in Canada, is one of the tallest mass timber structures in the world. However, the fire risk of wood is still a primary safety concern because of its combustible nature. For instance, a recent fire in Shuri Castle severely destroyed the wooden structure of this UNESCO World Heritage site in Okinawa, Japan (Fig. 1c). Despite many advanced fire preventive measures[7–9], the fire accidents of wooden structures have continuously raised their fire safety to be a public concern. Therefore, it is critical to understand the fire dynamics of wood to guide the fire safety design and optimize the emergency response.

Fig. 1. Photos of (a) the reconstruction of the wooden Neolithic Long House (courtesy: Czekaj Zastawny), (b) Brock Commons Tallwood House at the University of British Columbia in Canada (courtesy: Brudder), (c) Shuri Castle Fire in Japan in 2019 (courtesy: Robert Eldridge).

The ignition of wood can lead to the initiation and development of devastating fire events and is fundamental to fire safety analyses[10–12]. Therefore, since the 1960s, there is more than half a century of history in the development of both comprehensive and practical ignition theories of wood materials[13]. As a typical charring material, wood can sustain both flaming and smoldering combustion[14–17]. From both experiments and numerical simulations, the minimum heat flux for ignition is often the quantity of interest, and it is evident that both extrinsic and intrinsic factors may affect the ignition thresholds[18–23]. For piloted flaming ignition, a minimum heat flux of 12.5 kW/m^2 introduced by McGuire[24] in 1965 has been used for design purposes in many countries[13]. However, lower values have been subsequently found due to the improvement of experimental accuracy (e.g., 7.5 kW/m^2 suggested by Spearpoint[25]). For auto flaming ignition, a value of 20-25 kW/m^2 is a representative minimum heat flux for short-term irradiation exposures (minutes)[13,26]. However, when heated at lower levels for a longer period (hours), evidence has shown that wood will be eventually auto-ignited[27], but smoldering is generally first initiated and then transitions to flaming[28]. For example, Boonmee and Quintiere[29,30] reported that smoldering or glowing ignition was first achieved under irradiation between 10 kW/m^2 and 40 kW/m^2 before auto flaming ignition. Spearpoint[25] also reported the glowing ignition before flaming auto-ignition under irradiations less than 10 kW/m^2 if the wood was exposed for hours, rather than minutes.

Smoldering is the slow, low-temperature and flameless burning of porous fuel, and one of the most persistent types of combustion phenomena[31–33]. It is a heterogeneous process sustained when oxygen

molecules directly attack the hot surface of the reactive porous media, different from flame regarding combustion chemistry and transport process[31]. Smoldering can lead to fatal conditions due to its concealment, persistence and high lethal CO emissions[34]. However, only a limited number of experimental studies were reported on smoldering ignition at low heat fluxes[35,36]. Boonmee and Quintiere[30] observed the smoldering ignition at 10 kW/m^2 for 2 h and thus suggested 10 kW/m^2 to be the minimum heat flux of smoldering ignition. Gratkowski et al.[36] experimentally determined the minimum heat flux for smoldering ignition to be 7.5 kW/m^2, which was consistent with that of 7.2 kW/m^2 predicted by the self-heating theory. Yang et al.[37] further summarized the criteria of smoldering (or glowing) ignition for wood.

For the most natural and engineered woods, after flaming ignition, the flame is sometimes not able to self-sustain without strong irradiation (>40 kW/m^2), i.e., self-extinction may occur[14,38–42]. It is mainly because wood is almost impermeable to ambient oxygen, and only limited oxygen can diffuse through porous char layer[13]. For example, Ohlemiller[43] reported that wood needed a continuous irradiation of about 10 kW/m^2 to maintain smoldering. However, to the best of the authors' knowledge, few studies have investigated the limiting conditions for the self-sustained smoldering fire of wood materials.

This work aims to quantify the threshold of the self-sustained smoldering wood fire. Smoldering ignition tests are performed on natural beech wood blocks under low irradiation from 5 kW/m^2 to 10 kW/m^2 with different heating durations (up to 6 h). The required minimum heat flux, heating duration, temperature, and burning flux, as well as the emission characteristics, are quantified and analyzed to provide a full picture of smoldering ignition and near-limit burning behaviors of wood fires.

2. Experimental methods

The natural beech wood (a typical softwood with a Latin name of 'Zelkova Schneideriana'), which has the dimension of 100 mm × 100 mm × 60 mm, was tested in this study (Fig. 2a). The TG-DSC thermal analysis data is shown in Appendix. Before the tests, all wood samples were first dried at 90 °C in an oven for 48 h, and the dry bulk density was measured to be 650 ± 10 kg/m^3. Note that under long-term heating, the wood would be further dried before ignition, so the initial drying process and absorption of ambient water vapor were less relevant. Afterwards, all dried wood samples were placed into a dry cabinet to prevent the re-absorption of moisture from the ambient.

All the tests were conducted using the cone calorimeter (FTT I-Cone Plus), which mainly consisted of a conical heater, a sample holder, and a precision scale, as illustrated in Fig. 2b. The conical heater could provide relatively constant and uniform irradiation to the sample area of 100 mm × 100 mm, thus ensuring that the whole exposed surface of the wood sample would receive uniform irradiation[44,45]. Before the tests, the irradiation level was measured by a radiometer that was further calibrated by the temperature of the conical heater. The periphery and bottom of the wood sample were wrapped by 10-mm thick insulation of mineral wool, so the camera could not directly observe the sample burning process from the side. On the other hand, the top surface was exposed to the ambient and cone

irradiation, as shown in Fig. 2.

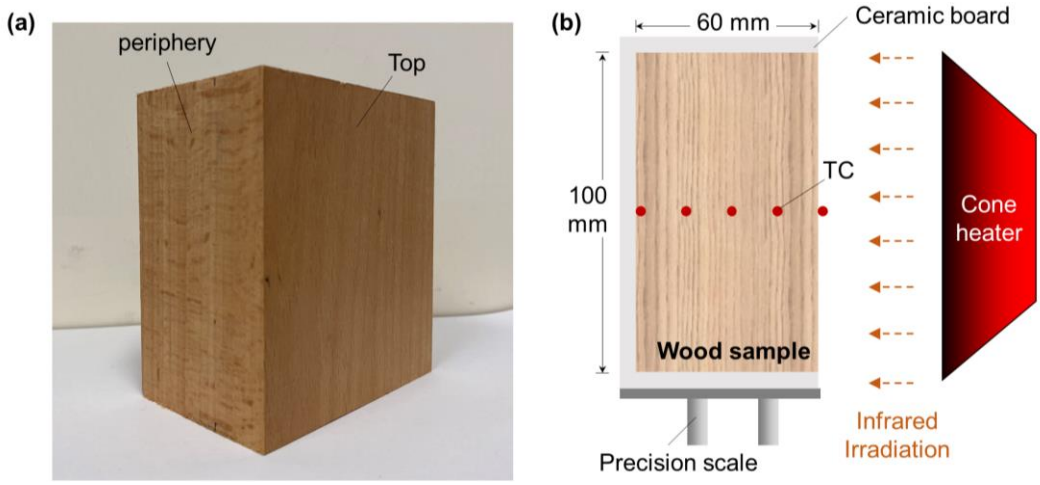

Fig. 2. (a) A photo of the wood sample used in this study, and (b) schematic experimental setup.

Initially, irradiation was shielded by the standard shutter, and the sample was installed on the precision scale where the unwrapped surface was exposed to the vertically oriented conical heater. In preliminary tests using the horizontal cone heater and wood sample, we found that the hot cone could pilot the uprising pyrolysis gases to cause flaming ignition. To prevent piloted flaming, the vertical heating test was conducted. The sample was heated across the grain.

Once the steel shield was removed, the prescribed irradiation was applied to the exposed wood surface. The cone irradiation varied from 5 kW/m^2 to 10 kW/m^2. Before tests, careful calibration was conducted for cone temperature and heat flux gauge under these low heat fluxes. Once the required heat flux was set, the cone temperature only varied within ± 5 °C, and the uncertainty of heat flux was less than ± 0.2 kW/m^2. Two groups of low-irradiation tests were designed:

(i) Continuous irradiation was applied on the wood surface until the end of the tests to observe the irradiation-assisted smoldering process and find out the critical heat flux for ignition, and

(ii) Irradiation was applied for a prescribed duration and then terminated to observe whether the smoldering fire became self-sustained.

To capture the temperature evolution and trace the position of smoldering front, five sheathed K-type thermocouples with a bead diameter of 1 mm were inserted into the central line at different depths of 0 mm (surface), 15 mm, 30 mm, 45 mm and 60 mm below the exposed surface, approximately. The test process was recorded by a side-view camera, and the sample mass was monitored by the precision scale (± 0.1 mg). All the emissions originated from wood smoldering were collected by an upper hood, and a partially exhaust stream with the flowrate of 1.5 ± 0.3 L/min were extracted from the hood by a sampling pump, for which a gas analyzer (Testo-430) was adopted to measure the gaseous emissions of CO and CO_2. During the test, the ambient temperature was maintained at 25 ± 2 °C, while the relative humidity was kept at 50 ± 5%. For each test, at least two or three repeating experiments were performed for uncertainty analysis.

3. Results and discussion

3.1. Smoldering temperature and ignition map

Fig. 3(a-b) shows the temperature evolutions under continuous irradiations of 10 kW/m^2 and 6 kW/m^2 from the start of exposure to the radiant heater to initiation of smoldering combustion and eventually burn-out. Once combustion is initiated at the surface, the smoldering front starts to propagate inwards with peak temperatures higher than 500 °C. As the smoldering front gradually reaches the bottom of the wood sample and approaches the top surface of the mineral-wool insulation, the in-depth heat conduction inside the wood is reduced; thus, the temperature close to the bottom is increased.

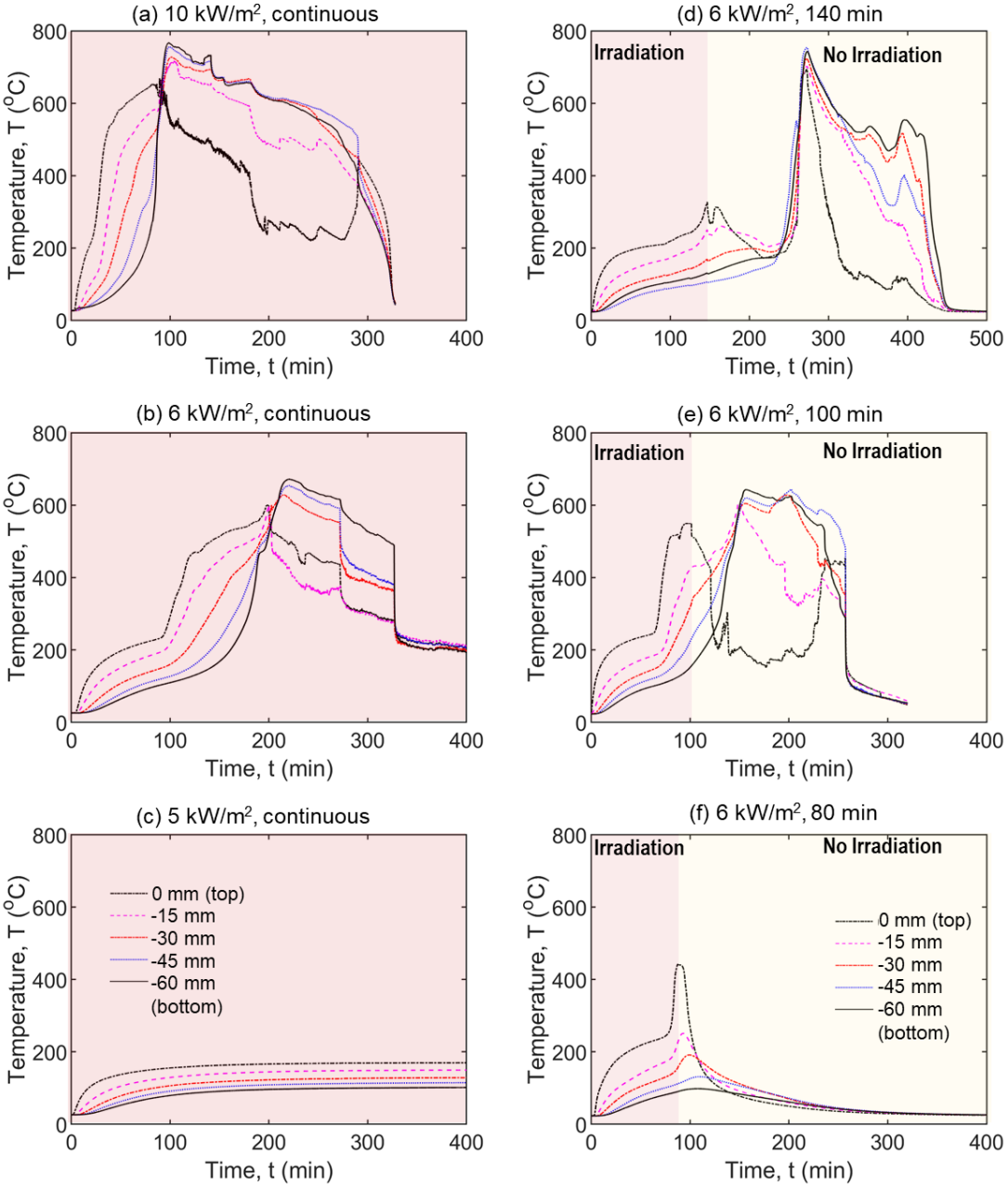

Fig. 3. Temperature profiles of smoldering wood under continuous irradiation of (a) 10 kW/m^2, (b) 6 kW/m^2 and (c) 5 kW/m^2, and under the irradiation of 6 kW/m^2 for (d) 140 min, (e) 100 min and (f) 80 min respectively, where the legends could be found in (c) or (f).

For example, in Fig. 3(b), after heating for 100 min, the smoldering front reaches the bottom of the wood sample and the peak temperature nearby (-60 mm) is over 700 °C, higher than that of 650 °C at -15 mm. After irradiation-assisted burning for more than 300 min, the fuel is burned out, and the temperature dramatically decreases. Comparatively, if the continuous irradiation is decreased to 5 kW/m^2, no ignition is achieved, as shown in Fig. 3(c). Eventually, the temperature profile reaches a steady state where the peak temperature is lower than 200 °C.

On the other hand, Fig. 3(d-f) show the temperature profiles of the wood samples where the irradiation of 6 kW/m^2 is shielded after applying on the wood surfaces for 140, 100 and 80 min, respectively. As shown in Fig. 3(d-e), once the irradiation is terminated at 140 min or 100 min, the temperature shows a slight fluctuation. Afterwards, the temperature re-increases and reaches a peak value of over 600 °C, indicating the existence of a self-sustained smoldering front. Eventually, the temperature decreases, and the fuel is completely burned out. Comparatively, in Fig. 3(f), after heating for 80 min, the temperature near the surface is higher than the smoldering ignition temperature of wood (~250 °C[13]). However, as the irradiation is shielded and terminated, smoldering cannot sustain itself, so the temperature drops to the ambient temperature.

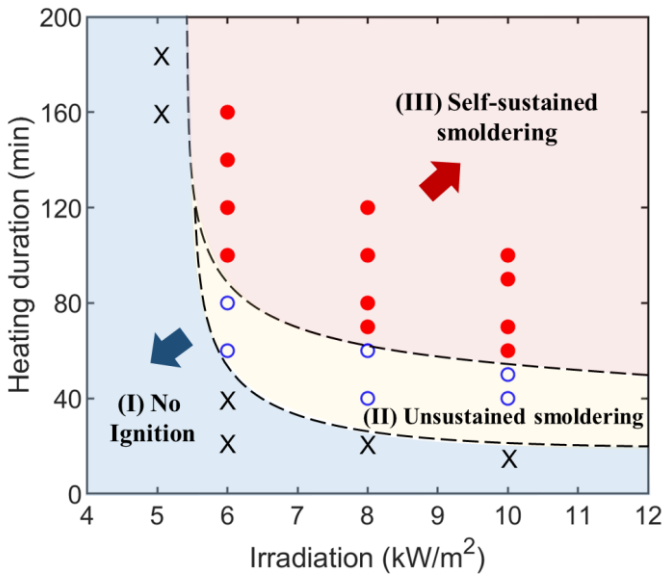

Fig. 4. Smoldering ignition map of woods, where the red solid circles and blue hollow circles represent the self-sustained smoldering and unsustained smoldering after removing irradiation, respectively.

By further plotting the experimental results in Fig. 4, a smoldering ignition map is obtained, where red solid circles and blue hollow circles represent self-sustained smoldering and no self-sustained smoldering after the removal of the external radiation, respectively. As the heating duration and heat flux increase, there are three regimes in the smoldering ignition map:

(I) No ignition,

(II) Unsustained smoldering, and

(III) Self-sustained smoldering.

First of all, the minimum heat flux for smoldering ignition of this wood sample is about 5.5±0.5 kW/m^2, lowering the ignition threshold of smoldering wood fire in the literature (as low as 7.5 kW/m^2)[11,30,36,43]. Moreover, to trigger a self-sustained smoldering fire, a longer heating duration is required, and the minimum heating duration decreases as the irradiation level increases. For example, as the irradiation increases from 6 kW/m^2 to 10 kW/m^2, the required heating duration decreases from 90±10 min to 55±5 min.

Fig. 5(a) shows the surface temperature of wood at the moment when the irradiation (6 kW/m^2) is just terminated. As expected, the surface temperature increases as the heating duration increases. After heating for 60 min or 80 min, the surface temperatures of both cases exceed 250 ºC, which is believed to be the minimum smoldering temperature of wood materials[13]. However, after the removal of the irradiation, smoldering is extinguished rather than becomes self-sustained. Further experiments demonstrated that, to ensure self-sustained smoldering, the surface temperature of the wood is required to be heated to over 350±20 ºC before the irradiation is terminated, which is much higher than the minimum smoldering ignition temperature[46].

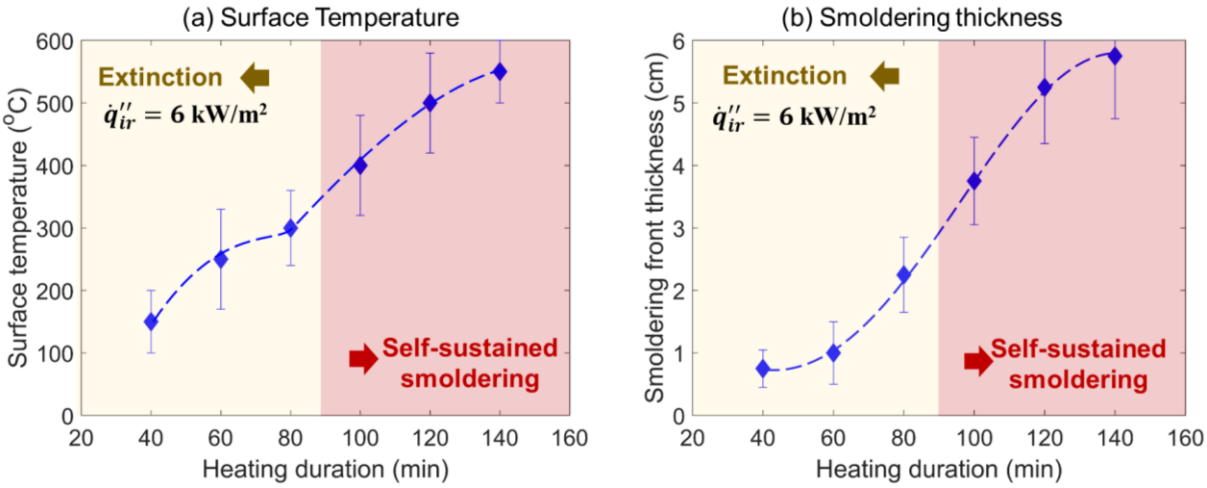

Fig. 5. (a) surface temperature and (b) thickness of smoldering front vs. irradiation duration (6 kW/m^2), where the markers represent the average values, and the error bars represent the standard deviations.

3.2. Smoldering front thickness

Given a minimum smoldering (char oxidation) temperature of 250 ºC[13,47], the average thickness of the smoldering front at the moment when the external radiation is terminated can be estimated based on the thermocouple data and the video recordings (e.g., Fig. 3). Fig. 5(b) summarizes the thickness of the smoldering front at different moments when the irradiation is removed, and it increases with the heating duration. For example, as the heating duration increases from 60 min to 140 min, the average smoldering front thickness increases from around 8 mm to 56 mm. More importantly, to trigger a self-sustained smoldering fire, the smoldering front should be extended over a thickness of about 30±5 mm before removing irradiation.

To better explain the necessity of a thick smoldering front for self-sustained smoldering propagation, a simplified energy conservation equation is applied to a propagating smoldering front with a thickness of δ, as illustrated in Fig. 6. On the limiting condition, to just sustain smoldering combustion, the heat generated from the smoldering zone due to the char oxidation ($\dot{q}''_{sm}$) should just overcome the heat loss to the ambient ($\dot{q}''_{\infty}$) and the heat conducted to the virgin wood ($\dot{q}''_{cond}$) as

$$\dot{q}''_{sm} \geq \dot{q}''_{\infty} + \dot{q}''_{cond} - \dot{q}''_{ir} \tag{1}$$

Under a long-term low-intensity heating ($\dot{q}''_{ir}$), the wood sample is near thermal equilibrium, and its internal temperature profile is almost linear (see Fig. 3c). Therefore, the in-depth conductive heat loss reaches a minimum constant ($\dot{q}''_{cond,min}$) as

$$\dot{q}''_{cond,min} = k\frac{T_{top} - T_{back}}{L} \tag{2}$$

where k is the thermal conductivity, T_{top} and T_{back} are the temperatures of top and back surfaces, and L is the thickness. The minimum surface temperature ($T_{top,min}$) is found to be about 350 °C, so the environmental heat loss ($\dot{q}''_{\infty}$) is also constant.

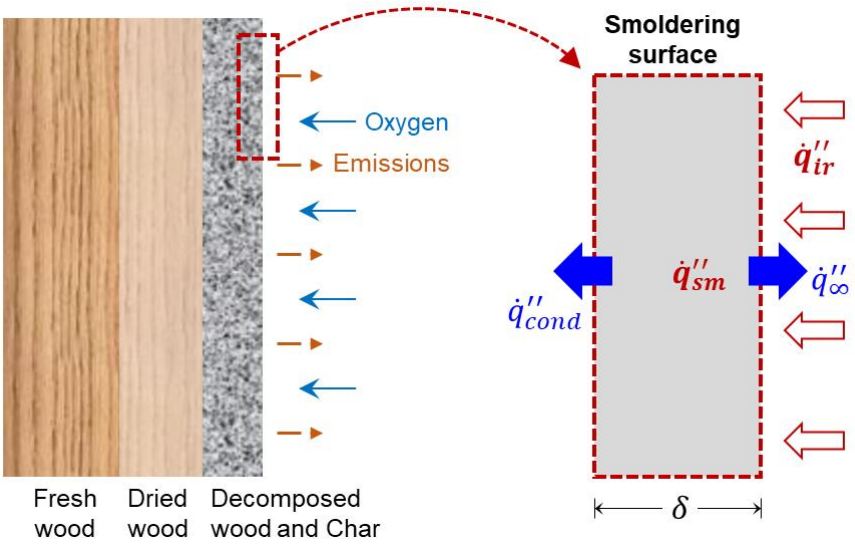

Fig. 6. Schematic diagram of the energy balance of a self-sustained smoldering front.

Then, when the irradiative heating is removed ($\dot{q}''_{ir} = 0$), to self-sustain the smoldering combustion, Eq. (1) could be revised as

$$\dot{q}''_{sm} = \dot{m}''_{sm}\Delta H_{sm} = \dot{q}''_{\infty} + \dot{q}''_{cond,min} \tag{3}$$

where $\dot{m}''_{sm}$ and ΔH_{sm} are the smoldering burning mass flux and the heat of the smoldering combustion. The burning mass flux is controlled by the overall smoldering reaction inside wood, so it is controlled by the temperature profile as

$$\dot{m}''_{sm} = \int_0^{\delta} \dot{\omega}'''_T dy \approx \delta_{min} \dot{\omega}'''_{sm} = \delta_{min} \rho Z \exp\left(-\frac{E}{RT_{sm}}\right) Y^n \quad (4)$$

where $\dot{\omega}'''_T$ is the volumetric reaction rate, δ_{min} is the minimum smoldering front thickness, ρ is the density of wood, Z is the pre-exponential factor, E is the activation energy, R is the universal gas constant, T_{sm} is the smoldering temperature, Y is the mass fraction of oxygen, n is the reaction order. Therefore, by defining a characteristic smoldering temperature of wood (T_{sm}), the minimum burning mass flux and front thickness of the self-sustained smoldering are both constants, expressed as

$$\dot{m}''_{sm} = \frac{\dot{q}''_{\infty} + \dot{q}''_{cond,min}}{\Delta H_{sm}} \quad (5)$$

$$\delta_{min} = \frac{\dot{q}''_{\infty} + \dot{q}''_{cond,min}}{\dot{\omega}'''_{sm} \Delta H_{sm}} \quad (6)$$

which successfully verify the experimental results in Fig 5(b) and Fig. 8.

3.3. Mass loss and burning mass flux

Fig. 7(a-b) shows the time evolutions of remaining mass (black solid line) and mass flux (red dashed line) of the same cases in Fig. 3(a-b) under continuous irradiation of 10 kW/m^2 and 6 kW/m^2. In general, these curves are similar to past studies of the flaming burning under cone calorimeter. For example, in Fig. 7(a), once the wood sample is exposed to the irradiation of 10 kW/m^2, the mass flux dramatically increases to about 6 g/m^2-s, indicating a robust smoldering burning process. Afterwards, the mass flux slightly decreases because the expanding char layer weakens the external heating from the conical heater.

As the smoldering front gradually reaches the top surface of the insulation board (see temperature profile in Fig. 3), the increased temperature due to the decreased heat conduction inside the wood sample promotes the smoldering process (see temperature profile in Fig. 3)[14,48]. Therefore, at about 75 min, the remaining mass witnesses a sharp decrease, while the mass flux re-increases to above 12 g/m^2-s. Afterwards, the mass flux decreases and only smolders at about 1 g/m^2-s because of the burning of residues. Fig. 7(c) shows an example of failed smoldering ignition of the wood sample under the low irradiation of 5 kW/m^2. Although the wood is heated for more than 400 min, the mass remains constant at about 380 g, and the mass flux is near zero.

On the other hand, Fig. 7(d-f) show the fuel mass and mass flux of wood samples where the irradiation of 6 kW/m^2 is shielded after applying on the wood surfaces for 140, 100 and 70 min, respectively. For example, as shown in Fig. 7(d), when the irradiation is terminated at 140 min, the mass flux starts to decrease. After fluctuation at the low level, the mass flux re-increases above 5 g/m^2-s. Afterwards, the mass flux decreases and remains at about 1 g/m^2-s due to the burning of residues. Comparatively, when the irradiation is terminated at 70 min, although the mass flux also reaches about 4 g/m^2-s, afterwards, the mass flux directly decreases to zero.

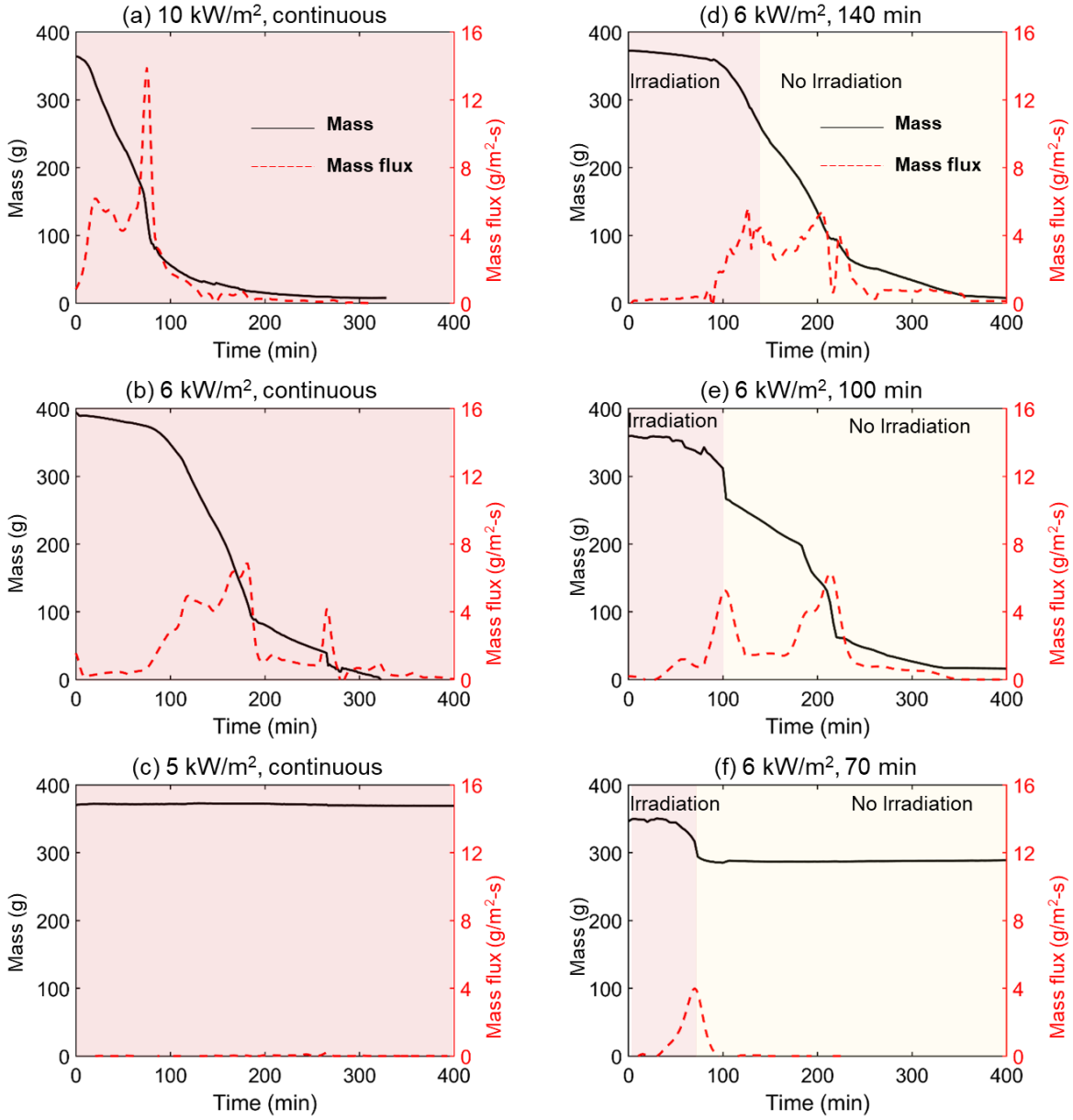

Fig. 7. Mass and mass flux of smoldering wood under continuous irradiation of (a) 10 kW/m^2, (b) 6 kW/m^2 and (c) 5 kW/m^2, and the mass and mass flux where the irradiation of 6 kW/m^2 was shielded after applying on the wood surfaces for (d) 140 min, (e) 100 min, and (f) 70 min, where the black solid lines and red dashed lines represent the mass and mass flux respectively.

Fig. 8 further summarizes the mass flux at the moment when the irradiation (6 kW/m^2) was terminated after different heating durations. As expected, the mass flux at the terminated moment increases as the heating duration increases. For example, the mass flux increases from 0.8 g/m^2-s to 5.5 g/m^2-s after irradiative heating for 40 min and 140 min, respectively. More importantly, to trigger a self-sustained smoldering, the mass flux should at least be increased to around 3.8±0.4 g/m^2-s before the removal of external radiation, which is almost consistent with the flame extinction limits (~4.0 g/m^2-s) of wood materials[39]. As seen from Eq. (5), a minimum burning flux ($\dot{m}''_{sm}$) is required to generate enough heat to overcome the heat loss to the ambient and the virgin fuels.

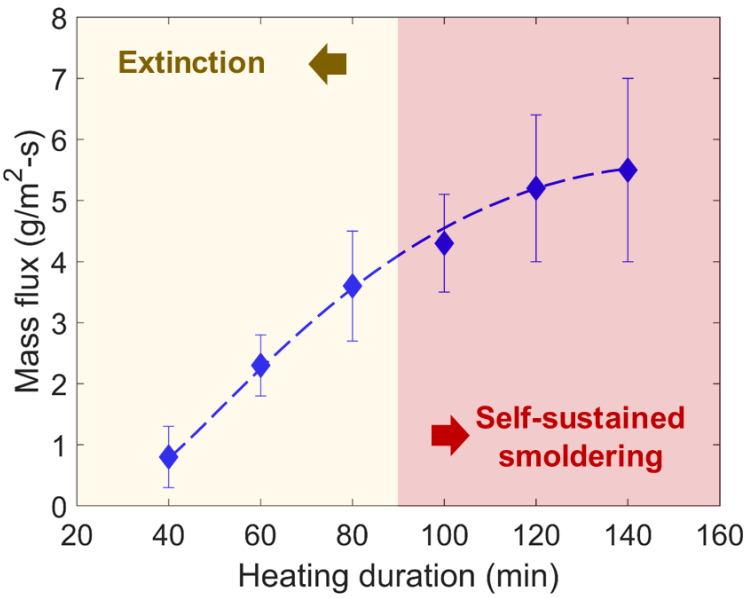

Fig. 8. The mass flux vs irradiation duration (6 kW/m^2), where the markers represent the average values, and the error bars represent the standard deviations.

3.4. Smoldering gas emissions

Fig. 9 shows the emission fluxes of CO_2 and CO of the same cases in Fig. 3, where the red and black lines represent the emissions of CO_2 and CO. Overall, these curves follow the same trends of mass flux data in Fig. 7, while the emission fluxes of CO_2 and CO vary with time simultaneously. For example, when the sample is continuously heated by irradiation of 10 kW/m^2, the emission fluxes of CO_2 and CO first increase to around 4 g/m^2-s and 1 g/m^2-s, as shown in Fig. 9(a). Afterwards, the fluxes almost remain stable and then re-increase to 10 g/m^2-s and 2 g/m^2-s at about 75 min, following the same trend in Fig. 7(a). For the case shown in Fig. 9(c), as no ignition was achieved, the emission fluxes are almost constant at zero for the whole process.

On the other hand, Fig. 9(d-f) also plot the emission fluxes of CO_2 and CO of the same cases in Fig. 3(d-f), where the irradiation of 6 kW/m^2 is terminated after applying for 140 min, 100 min and 80 min. For the cases of self-sustained smoldering, after the removal of irradiation, the emission fluxes of CO_2 and CO both slightly decrease but later re-increase, agreeing well with the mass flux evolution. For the case in Fig. 9(f), after the removal of irradiation, the emission flux directly drops to zero.

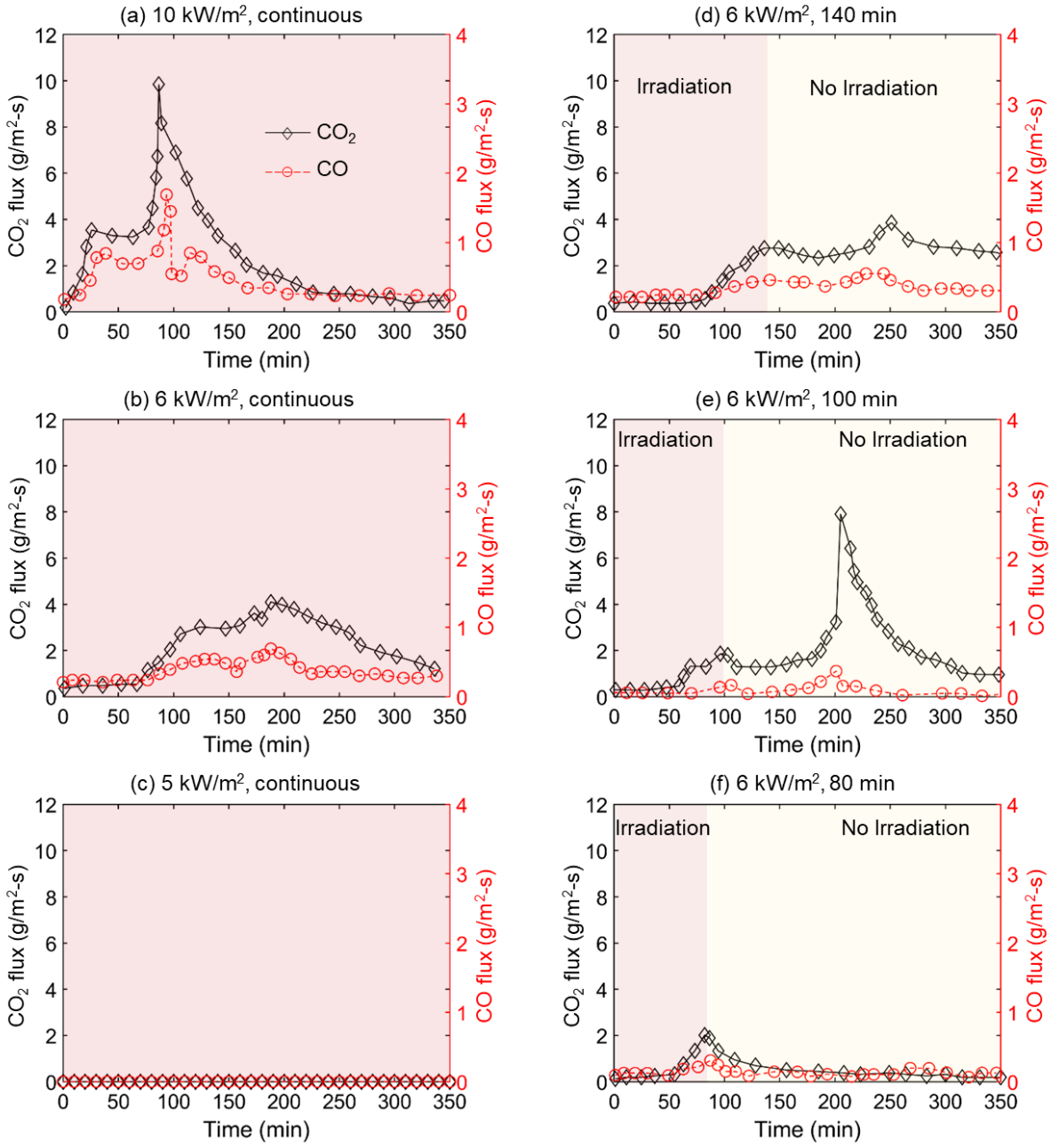

Fig. 9. The instantaneous emission fluxes of CO_2 (black) and CO (red) under continuous irradiation of (a) 10 kW/m^2, (b) 6 kW/m^2 and (c) 5 kW/m^2, and the emission fluxes of CO_2 and CO where the irradiation of 6 kW/m^2 was shielded after applying on the wood surfaces for (d) 140 min, (e) 100 min, and (f) 70 min, where the black solid lines and red dashed lines represent the CO_2 and CO respectively.

Fig. 10 further compares the CO/CO_2 ratio of the same cases in Fig. 9. In general, the peak CO/CO_2 during the smoldering combustion of this wood ranges from 0.1 to 0.2, which well agrees with the literature values[49–51] and is comparable to other combustible materials[16,49,52–59]. Moreover, from Fig. 10(a-b), CO/CO_2 ratio is found to slightly increase as the external radiation increases. On the other hand, after the removal of external radiation, if the smoldering front becomes self-sustained, the CO/CO_2 ratio eventually no longer vary with time for a long-lasting burning, as seen in Fig. 10(d-e).

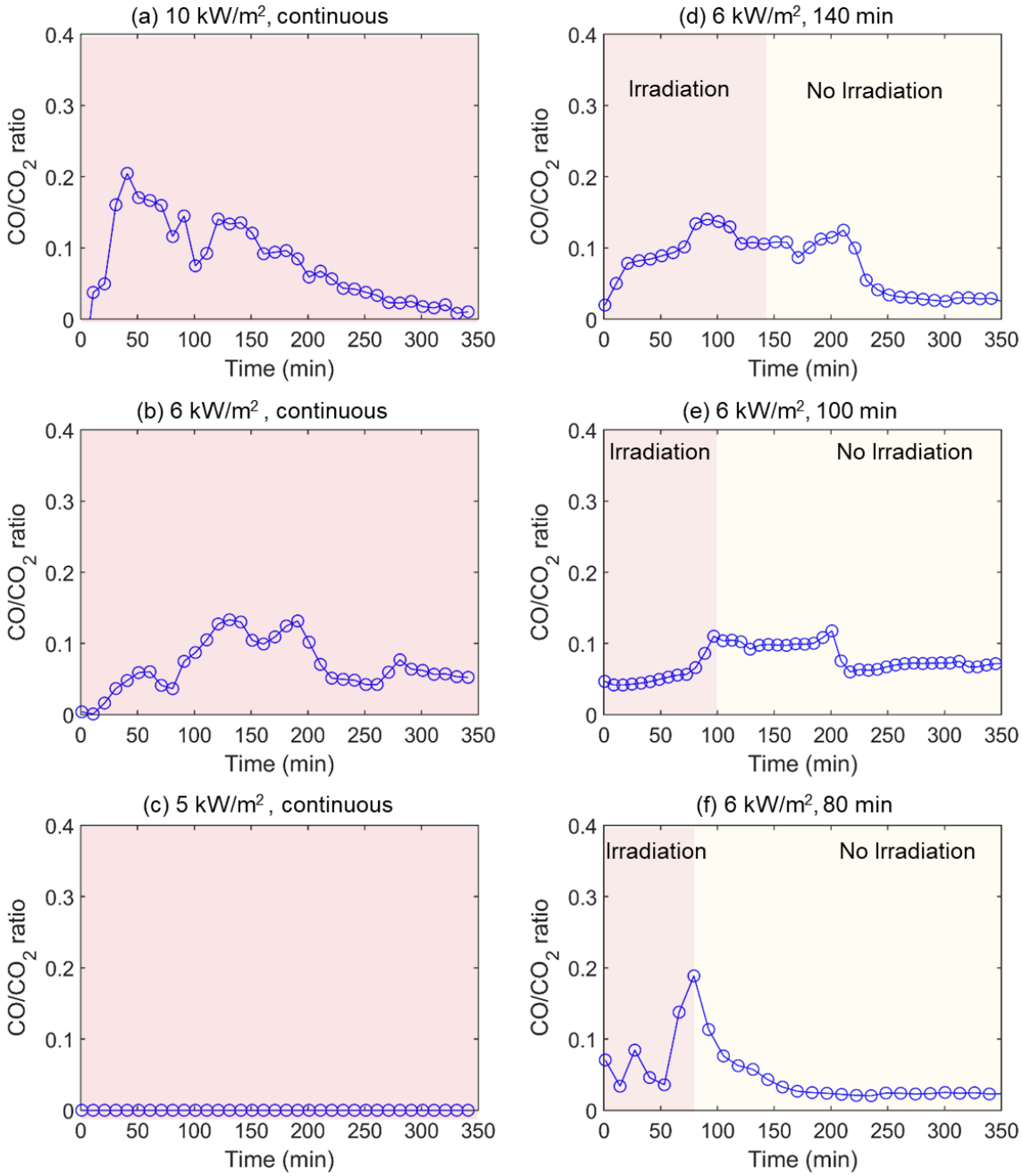

Fig. 10. The instantaneous CO/CO_2 ratio under continuous irradiation of (a) 10 kW/m^2, (b) 6 kW/m^2 and (c) 5 kW/m^2, and the CO/CO_2 ratio where the irradiation of 6 kW/m^2 was shielded after applying on the wood surfaces for (d) 140 min, (e) 100 min and (f) 70 min, respectively.

Note that the smoldering gas emissions obtained from the current study were obtained in the Cone Calorimeter, where ventilation was not restricted. Care should be exercised in applying the findings to fire situations, since in many cases the combustion of wood will be occurring under ventilation-limited conditions, leading to greater emissions of CO.

4. Conclusions

In this work, we use experimental approaches to investigate the smoldering ignition limits of woods

(beech woods) and quantify the necessary conditions to trigger a self-sustained smoldering front after the removal of external radiation. In previous, the minimum heat flux to initiate smoldering wood fire has been rarely studied, and the existing values are as low as 7.5 kW/m^2, close to the minimum heat flux of the pilot flaming ignition. However, we found that the minimum radiant heat flux for smoldering ignition is about 5.5 kW/m^2 after exposure to the low irradiation for hours. This minimum irradiation level lowers the required ignition boundary of smoldering combustion defined in the past literature.

We found a smoldering ignition map showing three different regimes, (I) no ignition, (II) unsustained smoldering and (III) self-sustained smoldering, depending on the irradiation intensity and heating duration. After ignition, the smoldering of wood may not self-sustain in the absence of irradiation. Such a self-extinction of smoldering is similar to the self-extinction of flame on wood. The self-sustained smoldering on thick wood without irradiation requires a longer and in-depth preheating process. The criteria for self-sustained smoldering wood include the minimum surface temperature of 350±20 ºC, the minimum smoldering front thickness of 30±5 mm, and the minimum mass flux of 3.8 ±0.4 g/m^2-s before the irradiation is removed.

The emission fluxes of CO_2 and CO are found to follow the same trends of mass flux evolutions. The CO/CO_2 ratio of the smoldering wood fire ranges from 0.1 to 0.2, consistent with the literature data. This work helps evaluate the fire risk and provides a better understanding of near-limit burning behaviors of wood materials under real fire scenarios. In our future work, additional testings and analyses of other wood species are needed to generalize the results of this study, and numerical simulations will be performed to reveal the underlying physical and chemical process of smoldering ignition under low irradiations.

Declaration of competing interest

The authors declare that they have no known competing financial interests or personal relationships that could have appeared to influence the work reported in this paper.

Acknowledgements

This work is funded by the National Natural Science Foundation of China (NSFC No. 51876183). The authors thank Mr Yunzhu Qin and Ms Yuying Chen (PolyU) for assistance in tests.

References

1. Karlen, C. Multiple Scales Insight into Using Timber for a Sustainable and Future Approach to Buildings. in *The Importance of Wood and Timber in Sustainable Buildings* (ed. Sayigh, A.) 195–211 (Springer Nature, 2021). doi:10.1007/978-3-030-71700-1_8.
2. Song, J. *et al.* Processing bulk natural wood into a high-performance structural material. *Nature*

554, 224–228 (2018).

3. Richard, B. Long houses, long mounds and Neolithic enclosures. *Journal of Material Culture* **1**, 239–256 (1996).
4. Brandner, R., Flatscher, G., Ringhofer, A., Schickhofer, G. & Thiel, A. Cross laminated timber (CLT): overview and development. *European Journal of Wood and Wood Products* **74**, 331–351 (2016).
5. Frangi, A., Fontana, M., Hugi, E. & Jübstl, R. Experimental analysis of cross-laminated timber panels in fire. *Fire Safety Journal* **44**, 1078–1087 (2009).
6. Liu, J. & Fischer, E. C. Review of large-scale CLT compartment fire tests. *Construction and Building Materials* **318**, 126099 (2022).
7. Hu, H. *et al.* Flammability and flame spread behavior of common fuels in Chinese historical buildings: An experimental research. *Combustion Science and Technology* (2022) doi:10.1080/00102202.2022.2050717.
8. Richter, F., Kotsovinos, P., Rackauskaite, E. & Rein, G. Thermal Response of Timber Slabs Exposed to Travelling Fires and Traditional Design Fires. *Fire Technology* (2020) doi:10.1007/s10694-020-01000-1.
9. Barber, D. Tall Timber Buildings: What's Next in Fire Safety ? *Fire Technology* **51**, 1279–1284 (2015).
10. Wang, S., Lin, S., Liu, Y., Huang, X. & Gollner, M. J. Smoldering ignition using a concentrated solar irradiation spot. *Fire Safety Journal* **129**, (2022).
11. Wang, S., Ding, P., Lin, S., Gong, J. & Huang, X. Smoldering and Flaming of Disc Wood Particles Under External Radiation: Autoignition and Size Effect. *Frontiers in Mechanical Engineering* **7**, 1–11 (2021).
12. Janssens, M. Piloted Ignition of Wood: *Fire and Materials* **15**, 151–167 (1991).
13. Babrauskas, V. Ignition fo Wood: A Review of the State of the Art. *Journal of Fire Protection Engineering* **12**, 163–189 (2001).
14. Lin, S., Huang, X., Gao, J. & Ji, J. Extinction of Wood Fire: A Near-Limit Blue Flame Above Hot Smoldering Surface. *Fire Technology* **58**, 415–434 (2022).
15. Lin, S. & Huang, X. Extinction of Wood Fire: Modeling Smoldering and Near-Limit Flame Under Irradiation. *Fire Technology* (2022) doi:10.1007/s10694-022-01295-2.

16. Lin, S., Sun, P. & Huang, X. Can peat soil support a flaming wildfire? *International Journal of Wildland Fire* **28**, 601–613 (2019).
17. Wang, S., Ding, P., Lin, S., Huang, X. & Usmani, A. Deformation of wood slice in fire: Interactions between heterogeneous chemistry and thermomechanical stress. *Proceedings of the Combustion Institute* **38**, 5081–5090 (2021).
18. Wesson, H. R., Welker, J. R. & Sliepcevich, C. M. The piloted ignition of wood by thermal radiation. *Combustion and Flame* **16**, 303–310 (1971).
19. Moghtaderi, B., Novozhilov, V., Fletcher, D. F. & Kent, J. H. A New Correlation for Bench-scale Piloted Ignition Data of Wood. *Fire Safety Journal* **29**, 41–59 (2006).
20. Mcallister, S. & Finney, M. Autoignition of wood under combined convective and radiative heating. *Proceedings of the Combustion Institute* **36**, 3073–3080 (2017).
21. Yafei, W. *et al.* Experiment study of the altitude effects on spontaneous ignition characteristics of wood. *Fuel* **89**, 1029–1034 (2010).
22. McAllister, S. Critical mass flux for flaming ignition of wet wood. *Fire Safety Journal* **61**, 200–206 (2013).
23. Simms, D. L. & Law, M. The ignition of wet and dry wood by radiation. *combustion and flame* **11**, 377–388 (1967).
24. McGuire, J. H. Fire and the spatial separation of buildings. *Fire Technology* **1**, 278–287 (1965).
25. Spearpoint, M. J. Predicting the ignition and burning rate of wood in the cone calorimeter using an integral model. (University of Maryland, 1999).
26. Quintiere, J. G. *Fundamentals of fire phenomena*. *Fundamentals of Fire Phenomena* (John Wiley, 2006). doi:10.1002/0470091150.
27. Schaffer, E. L. Smoldering initiation in cellulosics under prolonged low-level heating. *Fire Technology* **16**, 22–28 (1980).
28. Santoso, M. A., Christensen, E. G., Yang, J. & Rein, G. Review of the Transition From Smouldering to Flaming Combustion in Wildfires. *Frontiers in Mechanical Engineering* **5**, (2019).
29. Boonmee, N. & Quintiere, J. G. Glowing ignition of wood: The onset of surface combustion. *Proceedings of the Combustion Institute* **30 II**, 2303–2310 (2005).
30. Boonmee, N. & Quintiere, J. G. Glowing and flaming autoignition of wood. *Proceedings of the*

Combustion Institute **29**, 289–296 (2002).

31. Rein, G. Smoldering Combustion. *SFPE Handbook of Fire Protection Engineering* **2014**, 581–603 (2014).
32. Ohlemiller, T. J. T. J. Modeling of smoldering combustion propagation. *Progress in Energy and Combustion Science* **11**, 277–310 (1985).
33. Babrauskas, V. *Smoldering Fires*. (Fire Science Publishers, 2021).
34. Quintiere, J. *Principles of Fire Behaviour*. (Alar Elken, 1997).
35. Swann, J., Hartman, J. & Beyler, C. Study of Radiant Smoldering Ignition of Plywood Subjected to Prolonged Heating Using the Cone Calorimeter, TGA, and DSC. in *FIRE SAFETY SCIENCE–PROCEEDINGS OF THE NINTH INTERNATIONAL SYMPOSIUM* 155–166 (2008).
36. Gratkowski, M. T., Dembsey, N. A. & Beyler, C. L. Radiant smoldering ignition of plywood. *Fire Safety Journal* **41**, 427–443 (2006).
37. Yang, J., Hamins, A., Dubrulle, L. & Zammarano, M. Experimental and computational study of glowing ignition of wood. 1–13 (2021) doi:10.14264/cf558d0.
38. J.Hurley, M. & SFPE. *SFPE Handbook of Fire Protection Engineering*. *Springer* (Springer).
39. Emberley, R., Inghelbrecht, A., Yu, Z. & Torero, J. L. Self-extinction of timber. *Proceedings of the Combustion Institute* **36**, 3055–3062 (2017).
40. Arnórsson, S. M., Hadden, R. M. & Law, A. The Variability of Critical Mass Loss Rate at Auto-Extinction. *Fire Technology* (2020) doi:10.1007/s10694-020-01002-z.
41. Cuevas, J., Torero, J. L. & Maluk, C. Flame extinction and burning behaviour of timber under varied oxygen concentrations. *Fire Safety Journal* 23 (2020) doi:10.1016/j.firesaf.2020.103087.
42. Bartlett, A. I. *et al.* Auto-extinction of engineered timber: Application to compartment fires with exposed timber surfaces. *Fire Safety Journal* **91**, 407–413 (2017).
43. Ohlemiller, T. J. *Smoldering combustion*. (1986).
44. Lindholm, J., Brink, A. & Hupa, M. Cone calorimeter – a tool for measuring heat release rate. *Finnish-Swedish Flame Days 2009* 4B (2009) doi:10.1002/fam.
45. Babrauskas, V. The Cone Calorimeter. in *SFPE Handbook of Fire Protection Engineering* (ed. Hurley, M.) 952–980 (Springer, 2016). doi:10.1007/978-1-4939-2565-0.
46. Babrauskas, V. Journal of Fire Protection Ignition of Wood : A Review of the State of the Art. *Journal of Fire Protection Engineering* **12**, 163–189 (2002).

47. Lin, S. & Huang, X. Quenching of smoldering: Effect of wall cooling on extinction. *Proceedings of the Combustion Institute* **38**, 5015–5022 (2021).

48. Huang, X., Li, K. & Zhang, H. Modelling bench-scale fire on engineered wood: Effects of transient flame and physicochemical properties. *Proceedings of the Combustion Institute* **36**, 3167–3175 (2017).

49. Malow, M. & Krause, U. Smouldering combustion of solid bulk materials at different volume fractions of oxygen in the surrounding gas. *Fire Safety Science* **9**, 303–314 (2008).

50. Tsuchiya, Y. CO/CO2 Ratios in Fire. *Fire Safety Science-Proceedings of the Fourth International Symposium* 515–526 (1994).

51. Cobian-Iñiguez, J. *et al.* Wind Effects on Smoldering Behavior of Simulated Wildland Fuels. *Combustion Science and Technology* **00**, 1–18 (2022).

52. Yokelson, R. J., Susott, R., Ward, D. E., Reardon, J. & Griffith, D. W. T. Emissions from smoldering combustion of biomass measured by open-path Fourier transform infrared spectroscopy. *Journal of Geophysical Research* **102**, 18865 (1997).

53. Hu, Y., Christensen, E., Restuccia, F. & Rein, G. Transient gas and particle emissions from smouldering combustion of peat. *Proceedings of the Combustion Institute* **37**, 4035–4042 (2019).

54. Putzeys, O., Fernandez-Pello, C., Gein, G. & Urban, J. L. The piloted transition to flaming in smoldering fire retarded and non-fire retarded polyurethane foam. *Fire and Materials* **32**, 485–499 (2008).

55. Nazım, U. Investigation of Fire Behavior of Rigid Polyurethane Foams Containing Fly Ash and Intumescent Flame Retardant by Using a Cone Calorimeter. *Journal of Applied Polymer Science* **124**, 3372–3382 (2011).

56. Stec, A. A. & Hull, T. R. Assessment of the fire toxicity of building insulation materials. *Energy and Buildings* **43**, 498–506 (2011).

57. Wang, H. *et al.* Smouldering fire and emission characteristics of Eucalyptus litter fuel. *Fire and Materials* **46**, 576–586 (2022).

58. Huang, H. L., Lee, W. M. G. & Wu, F. S. Emissions of air pollutants from indoor charcoal barbecue. *Journal of Hazardous Materials* **302**, 198–207 (2016).

59. He, F. & Behrendt, F. Experimental investigation of natural smoldering of char granules in a packed bed. *Fire Safety Journal* **46**, 406–413 (2011).

Appendix

The wood sample was first pulverized into powders and dried at 90 °C for 48 h. The thermal analysis of the wood sample was performed using a PerkinElmer STA 6000 Simultaneous Thermal Analyzer in an air atmosphere (21% oxygen). The initial mass was around 3 mg, and the sample was heated at a relatively low heating rate of 5 K/min. Fig. A1 shows the mass-loss rate and the heat flow curves of this beech wood. As expected, the mass loss rate rapidly increases at about 250 °C, which could be defined as the pyrolysis temperature.

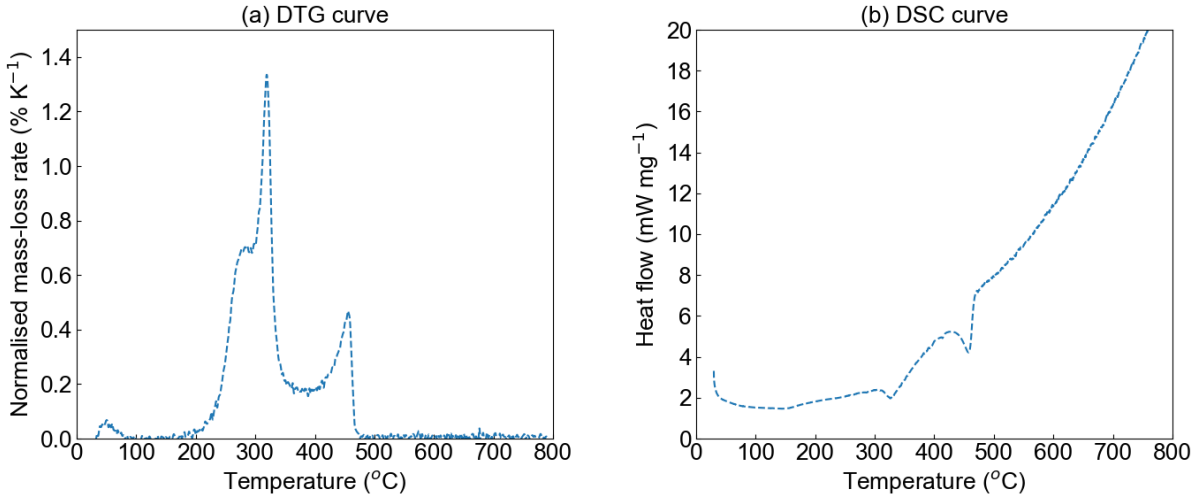

Fig. A1. TGA-DSC results of the beech wood sample under air at a heating rate of 5 K/min.